

Hole-doped semiconductor nanowire on top of an s -wave superconductor: A new and experimentally accessible system for Majorana fermions

Li Mao¹, Ming Gong¹, E. Dumitrescu², Sumanta Tewari², and Chuanwei Zhang^{1*}
¹*Department of Physics and Astronomy, Washington State University, Pullman, WA 99164 USA*
²*Department of Physics and Astronomy, Clemson University, Clemson, SC 29634 USA*

Majorana fermions were envisioned by E. Majorana in 1935 to describe neutrinos. Recently it has been shown that they can be realized even in a class of electron-doped semiconductors, on which ordinary s -wave superconductivity is proximity induced, provided the time reversal symmetry is broken by an external Zeeman field above a threshold. Here we show that in a hole-doped semiconductor nanowire the threshold Zeeman field for Majorana fermions can be very small for some *magic* values of the hole density. In contrast to the electron-doped systems, smaller Zeeman fields and much stronger spin-orbit coupling and effective mass of holes allow the hole-doped systems to support Majorana fermions in a parameter regime which is routinely realized in current experiments.

PACS numbers: 74.78.-w, 03.67.Lx, 71.10.Pm, 74.45.+c

Recently some exotic condensed matter systems, such as the Pfaffian states in fractional quantum Hall (FQH) systems [1–4], chiral p -wave superconductors/superfluids [5–9], topological insulator (TI) [10], as well as a ferromagnet-superconductor heterostructure [11], have been proposed as systems supporting quasiparticles with non-Abelian statistics [12]. These systems allow a special type of quasiparticles called Majorana fermions which involve no energy cost. The second quantized operators γ_i for the Majorana excitations are self-hermitian, $\gamma_i^\dagger = \gamma_i$ (particles are their own anti-particles), which lies at the heart of their non-Abelian statistical properties. Due to the fundamental difference of Majorana fermions from any other known quantum particles in nature, the emergence of these particles in solid state systems would in itself be an extraordinary phenomenon. Their potential use in fault-tolerant topological quantum computation (TQC) [12] makes their realization in controllable solid state systems even more significant.

It has been shown recently [13–18] that an electron-doped semiconducting thin film or nanowire with a sizable spin-orbit coupling can host, under suitable conditions, Majorana fermion excitations localized near defects. This proposal followed on an earlier similar proposal in the context of cold atomic systems [19]. When the film or the nanowire is in the presence of a Zeeman splitting V_z (with Landé factor g_e^*) and an s -wave superconducting pair potential Δ , which can be proximity induced by a nearby superconductor, the system enters into a topological superconducting (TS) state for

$$V_z^2 > \Delta^2 + \mu^2, \quad V_z = g_e^* \mu_B B / 2 \quad (1)$$

Here μ is the chemical potential in the semiconductor which is controlled by the density of doped electrons. Despite the theoretical success, the requirement Eq. (1) for the TS state in an electron-doped nanowire leads to two obvious experimental challenges: a low electron density and a high magnetic field. For a small carrier density

a nanowire tends to become insulating due to the strong disorder-induced fluctuations of the chemical potential. A high magnetic field, on the other hand, can be detrimental to pairing as well as s -wave proximity effect itself.

In this Letter we show that a *hole-doped* semiconductor nanowire can solve all these problems encountered in the electron-doped systems. The hole-doped nanowire is very different in many respects from its electron-doped counterpart due to its different band structure and the value of the effective spin of the carriers. For some “magic” values of the carrier (hole) density the threshold Zeeman splitting for the TS states and Majorana fermions can become very small, therefore the constraint on the carrier density as given in Eq. (1) is absent for the hole-doped nanowires. Furthermore, the effective mass and spin-orbit coupling in the p -type *valence* band holes are much larger than electrons, which leads to a larger Fermi vector k_F . This larger k_F leads to a larger required carrier density ($\sim 10^6 \text{ cm}^{-1}$) for the TS state, which, remarkably, is now *routinely achieved* in many experiments [20–22]. The large carrier density provides strong screening of the disorder potentials, leading to much smaller fluctuations of the chemical potential [23] in the nanowire. Furthermore, the small ratio between the Zeeman coupling and the spin-orbit energy (orders of magnitude smaller than that in the electron-doped systems) leads to a small carrier mobility requirement for the hole-doped TS state (3 order of magnitude smaller than that for the electron-doped TS state), as pointed out recently in [24]. Let us also point out that the superconducting proximity effect on a hole-doped nanowire has been observed in recent experiments [22]. It seems therefore that a Majorana-carrying TS state is tantalizingly close to experimental reach in a hole-doped nanowire.

Set-up and Hamiltonian: The experimental setup is illustrated in Fig. 1a, where a hole-doped semiconductor nanowire is placed on top of an s -wave superconductor. We focus on large-band gap semiconductors, where the single particle Hamiltonian of holes is described by the

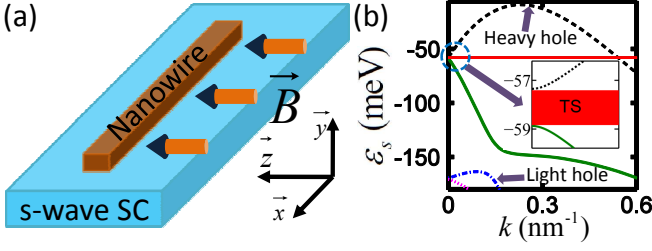


FIG. 1: (a) Schematic plot of the experimental setup. (b) Illustration of the valence band structure of 1D hole-doped nanowire with a Zeeman field. Only the lowest band along the y and z directions is considered. There are two heavy hole (dashed black and solid green curves) and two light hole (blue dash-dotted and pink dotted curves) bands. The thick red line (amplified as shadow in inset) gives the regime of chemical potential with a single Fermi surface, which leads to the topological superconducting state. The parameters are for a hole-doped InAs nanowire with $\gamma_1 = 20$, $\gamma_2 = 8.5$. $\alpha = 3.3 \times 10^5$ m/s, $V_z = 1.5$ meV, $L_z = 14$ nm, $L_y = 10$ nm.

four-band Luttinger model [25] (henceforth we set $\hbar = 1$, and $m = -1$),

$$H_L = \left(\frac{\gamma_1}{2} + \frac{5\gamma_2}{4}\right)\nabla^2 - \gamma_2(\nabla \cdot \mathbf{J})^2 - i\alpha(\mathbf{J} \times \nabla) \cdot \hat{z} + V_z J_z - \mu, \quad (2)$$

where α is the Rashba spin-orbit coupling due to the inversion-symmetry breaking, and the fourth term is the Zeeman field $V_z = g_h^* \mu_B B$ generated by the external magnetic field along the z direction. \mathbf{J} is the total angular momentum operator for a spin-3/2 hole, γ_1 and γ_2 are the Luttinger parameters. Note that here the relation between V_z and B differs from Eq. (1) by a factor 1/2 because we use the spin-3/2 matrix J_z , instead of the Pauli matrix which was used for Eq. (1) [13] (thus the required B for the same V_z is smaller by a factor 1/2).

To simplify the calculations we assume a rectangular cross-section of the nanowire with the widths L_y and L_z . The strong confinement along the y and z directions makes the energy levels quantized on these axes. To illustrate the emergence of the Majorana fermions, we first consider a single band, *i.e.*, the lowest energy state along the y and z directions. Using the ground state wavefunction $\phi(y, z)$ along the y and z directions, the original Hamiltonian (2) in 3D can be projected to an effective 1D form

$$H_1(x) = \left(\gamma_1/2 + 5\gamma_2/4 - \gamma_2 J_x^2\right) \partial_x^2 + \pi^2 \gamma_2 J_y^2 / L_y^2 + \pi^2 \gamma_2 J_z^2 / L_z^2 + i\alpha J_y \partial_x + V_z J_z - \xi - \bar{\mu}, \quad (3)$$

where $\xi = 5\gamma_2 \pi^2 (L_y^{-2} + L_z^{-2}) / 4$, and $\bar{\mu} = \mu + \gamma_1 \pi^2 (L_y^{-2} + L_z^{-2}) / 2$ is the shifted chemical potential due to the confinement.

In Fig. 1b, we plot the energy spectrum ε_s of the Hamiltonian (3) for holes in a 1D geometry. There are two heavy hole and two light hole bands. If μ lies in

the shaded region, it intercepts only one Fermi surface. An odd number of Fermi surfaces implies a breakdown of the fermion doubling theorem (due, in this case, to the Zeeman splitting), which yields, in the presence of a superconducting pair potential, the required TS state for Majorana fermions [10]. The position of the shaded region (the TS state) is determined by the Hamiltonian (3) at $k = 0$ that depends on the parameters γ_1 , γ_2 , L_y , L_z , while the width of the shaded region is determined by V_z . The large effective mass and strong spin-orbit coupling of the holes lead to a high density $n = \int_0^{k_F} dk / 2\pi \sim 10^6$ cm $^{-1}$ of holes in the TS state. Such a high density is routinely realized in nanowire experiments [20–22]. The high carrier density provides a strong screening of the disorder potential, suppressing the spatial chemical potential fluctuations and disorder effects [23].

The superconducting pair potential can be induced in the hole-doped nanowire through the proximity contact with an *s*-wave superconductor (Fig. 1a), as demonstrated in experiments [22]. This yields the Hamiltonian,

$$H_{sc} = \sum_{m_J} \int d^3 \mathbf{r} \Delta_{sm_J}(\mathbf{r}) \hat{\psi}_{m_J}^\dagger \hat{\psi}_{-m_J}^\dagger + \text{H.c.}, \quad (4)$$

where $\hat{\psi}_{m_J}^\dagger$ are the creation operators for holes with the angular momentum $m_J = \frac{1}{2}, \frac{3}{2}$ and $\Delta_{sm_J}(\mathbf{r})$ is the proximity induced pair potential. The form of the pairing Hamiltonian is dictated by the fact that Δ_{sm_J} couples particles with m_J with particles with $-m_J$, and should be determined through the microscopic theory of the proximity effect [26].

Taking account of the spin-3/2 and the particle-hole degrees of freedom in the superconductor, the Bogoliubov-de-Gennes (BdG) Hamiltonian can be written as an 8×8 matrix

$$\hat{H}_{\text{BdG}} = \begin{pmatrix} H_1(x) & \Delta_S(x) \\ \Delta_S^*(x) & -\Upsilon^\dagger H_1^*(x) \Upsilon \end{pmatrix} \quad (5)$$

in the Nambu spinor basis $\hat{\Phi}(x) = \left(\hat{\psi}(x), \Upsilon \hat{\psi}^\dagger(x)\right)^T$ with $\Upsilon = i(I_2 \otimes \sigma_x) \tau_y$ (I_2 is the 2×2 unit matrix), $\Delta_S(x) = \text{diag}(\Delta_{s3/2}, \Delta_{s1/2}, \Delta_{s1/2}, \Delta_{s3/2})$, and $\hat{\psi}(x) = (\hat{\psi}_{\frac{3}{2}}(x), \hat{\psi}_{\frac{1}{2}}(x), \hat{\psi}_{-\frac{1}{2}}(x), \hat{\psi}_{-\frac{3}{2}}(x))$.

Parameter space for the topological state: In a 1D nanowire, the parameter regime for the Majorana fermions (in 1D the Majorana fermions are localized at the two end points) can be determined by the topological index \mathcal{M} [27, 28] defined as,

$$\mathcal{M} = \text{sgn}[\text{Pf}\{\Gamma(0)\}] \text{sgn}[\text{Pf}\{\Gamma(\pi/a)\}]. \quad (6)$$

Here Pf represents the Pfaffian of the anti-symmetric matrix $\Gamma(k) = -iH_{\text{BdG}}(k)(\varsigma_y \otimes \Upsilon)$, ς_y is the Pauli matrix, $H_{\text{BdG}}(k)$ is the corresponding BdG Hamiltonian in the momentum space ($-i\partial_x \rightarrow k$), and a is the lattice constant. $\mathcal{M} = -1$ (+1) corresponds to the topologically nontrivial (trivial) states with (without) Majorana

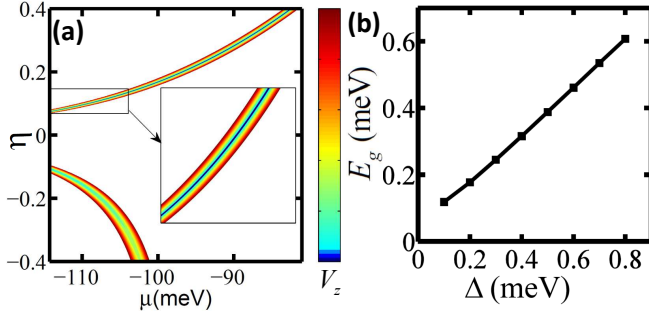


FIG. 2: (a) Plot of the phase boundary ($\mathcal{F} = 0$) between topological and non-topological states for different μ , V_z^c and η . $\Delta_{s1/2} = 1$ meV, $\beta_2 = 55.4$ meV (corresponding to $L_y = 10$ nm), $\beta_1 = (1 - \eta)/(2\sqrt{|\eta|})\sqrt{\beta_2^2 - \eta\Delta_{s1/2}^2}$. The color region represents the TS state with $M = -1$. Different colors correspond to different critical Zeeman fields. (b) Plot of the minigap E_g with respect to Δ . $\mu = -50.9$ meV, $V_z = 1.5$ meV, $L_y \approx 9$ nm and $L_z \approx 15$ nm.

fermions. Using the fact that $\Gamma(k)$ is an anti-symmetric matrix that can be diagonalized by a lower triangular matrix [29], we find

$$\text{Pf}\{\Gamma(k)\} = \text{Pf}\{\Delta_S \Upsilon\} \text{Pf}\{\Upsilon \Delta_S + H_1^T(k) \Upsilon \Delta_S^{-1} H_1(k)\} \quad (7)$$

through a straightforward calculation.

In the continuous limit $k = \pi/a \rightarrow \infty$, the k^2 terms in the single particle Hamiltonian $H_1(k)$ dominates and all other terms in $\Gamma(k)$ can be neglected. In this case, it can be shown that $\text{sgn}[\text{Pf}\{\Gamma(k)\}] = \text{sgn}[\det(H_1(k))] = 1$, therefore \mathcal{M} is solely determined by the sign of $\text{Pf}\{\Gamma(0)\}$. $\text{Pf}\{\Gamma(0)\}$ can be derived analytically from Eq. (7), yielding $\mathcal{M} = \text{sgn}[\mathcal{F}]$, where

$$\mathcal{F} = f_0 - f_1 V_z^2 + 9V_z^4/16, \quad (8)$$

$f_0 = (\bar{\mu}^2 + \Delta_{s3/2}\Delta_{s1/2} - \beta_1^2 - \beta_2^2)^2 + [(\Delta_{s3/2} - \Delta_{s1/2})\bar{\mu} + \beta_1(\Delta_{s3/2} + \Delta_{s1/2})]^2$, $f_1 = [10\bar{\mu}^2 + 10\beta_1^2 + 16\beta_1\bar{\mu} + 9\Delta_{s1/2}^2 + \Delta_{s3/2}^2 - 6\beta_2^2]/4$, $\beta_1 = \pi^2\gamma_2(L_z^{-2} - L_y^{-2}/2)$, $\beta_2 = \sqrt{3}\pi^2\gamma_2 L_y^{-2}/2$. Since \mathcal{M} changes sign when \mathcal{F} changes sign, the phase boundary between the topologically trivial and nontrivial states can be determined by setting $\mathcal{F} = 0$.

When the ratio $\eta = \Delta_{s3/2}/\Delta_{s1/2} \geq \Delta_{s3/2}^2/\beta_2^2$, there exists a magic value of the chemical potential $\bar{\mu}_0 = \frac{\eta+1}{4|\eta|}\sqrt{\eta\beta_2^2 - \Delta_{s3/2}^2}$ in the heavy hole band such that $f_0 = 0$, where $\beta_1 = (1 - \eta)\bar{\mu}_0/(1 + \eta)$. For $f_0 = 0$, $\mathcal{F} < 0$ and Majorana fermions exist even for a vanishingly small V_z . Clearly, $\eta \geq \Delta_1^2/\beta_2^2$ requires that $\Delta_{s3/2}$ and $\Delta_{s1/2}$ have the same sign and $\beta_2^2 \geq \Delta_1\Delta_2$. Because of the strong confinement, the second condition can be easily satisfied. Therefore the threshold Zeeman field V_z^c for the TS state vanishes when $\Delta_{s3/2}$ and $\Delta_{s1/2}$ are of the same sign, independent of their relative magnitudes. When $\Delta_{s3/2}$ and $\Delta_{s1/2}$ have different signs, V_z^c

becomes nonzero, but is still much smaller than that for the electron-doped semiconductors. Therefore the relative signs of the pair potentials should not matter in realistic experiments because a reasonable V_z is always needed to generate a sizable chemical potential region for the TS state. In Fig. 2, we plot the boundary $\mathcal{F} = 0$ between topologically trivial and non-trivial states for different μ , V_z^c and η . The TS states for a fixed V_z^c are embraced by two lines with the same color for the corresponding V_z^c . For instance, for $\eta = 0.15$ and $V_z^c = 1$ meV, Fig. 2 shows that the TS state exists in the region $\mu_1 < \mu < \mu_2$ with $\mu_1 = -103.3$ meV and $\mu_2 = -100.8$ meV. Clearly, the $V_z = 0$ line (the center blue line) exists for $\eta > 0$, but vanishes for $\eta < 0$. When $\eta \rightarrow 0^+$, $\bar{\mu}_0 \rightarrow -\infty$.

The vanishingly small V_z^c for the TS state at $\eta > 0$ may also be understood by projecting the four band Luttinger model in Eq. (3) to an effective two heavy hole band model because of the large energy splitting between the heavy and light hole bands. The resulting two band model is generally very complicated for finite k_x and V_z . However, because the Pfaffian is determined by the Hamiltonian at $k = 0$ and we are interested in the TS state with vanishingly small V_z , we can do the band projection at $V_z = 0$ and around $k_x = 0$, leading to an effective pairing $\Delta^{eff} = (\Delta_{s3/2} - \kappa\Delta_{s1/2})/\kappa$ and an effective chemical potential $\bar{\mu}_{eff} = \bar{\mu} - \sqrt{\beta_1^2 + \beta_2^2}$, with $\kappa = \left(\sqrt{\beta_1^2/\beta_2^2 + 1} - \beta_1/\beta_2\right)^2$. Here we have neglected non-diagonal term of the pairing because $\beta_2^2 \gg \Delta_{s3/2}\Delta_{s1/2}$. When $\eta > 0$, Δ^{eff} may vanish by choosing $\beta_1/\beta_2 = (1 - \eta)/2\sqrt{\eta}$, therefore the critical Zeeman field V_z^c also vanishes when $\bar{\mu}_{eff} = 0$. While when $\eta < 0$, Δ^{eff} is always finite and there is a minimum V_z^c based on Eq. (1) for the two-band model. Note that the zero Δ^{eff} at $k_x = 0$ and $V_z = 0$ does not imply the zero Δ at a finite V_z and k_x . For a large k_x , the coupling between heavy and light holes becomes important and the minigap is finite for a large V_z even at the magic μ_0 (see Fig. 3b).

Henceforth, we consider two representative cases to further illustrate our results: (I) $\Delta_{s3/2} = \Delta_{s1/2} = \Delta$ and (II) $\Delta_{s3/2} = -\Delta_{s1/2} = \Delta$. For the a reasonable large V_z , both pairings yield similar observable signals. The corresponding topological region is plotted in Fig. 3a. In the case (I), the TS states exist in the region $|\bar{\mu} - \bar{\mu}_0| \lesssim |V_z|/2$ for both positive and negative V_z . The transition at $V_z = 0$ (at which the superconductor is gapless and non-topological) is a quantum transition at which neither the symmetry of the system nor the topological properties change as a function of V_z . Note that the system crosses the phase transition boundary lines twice when V_z changes from $-\infty$ to $+\infty$ for a fixed $\bar{\mu}$, except at the magic value $\bar{\mu}_0$. At the phase boundary, the quasiparticle energy gap closes and the superconductor becomes gapless. At the magic $\bar{\mu}_0$, the two lines of

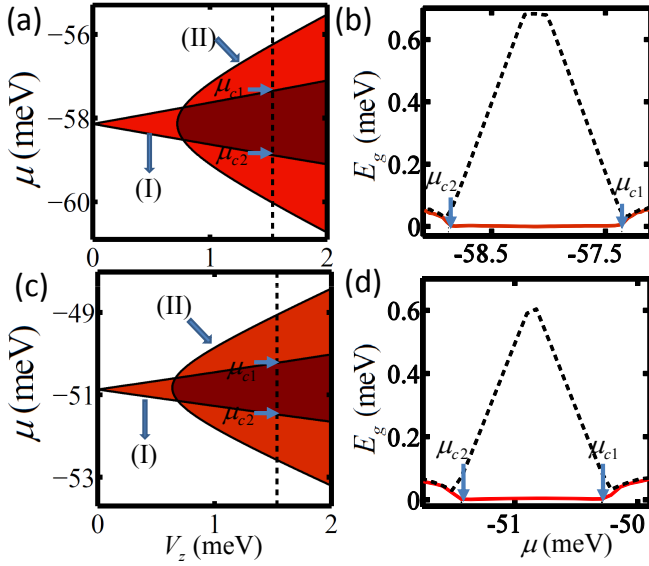


FIG. 3: The parameter regime for the existence of Majorana fermions. (a,b) and (c,d) correspond to the single and two band models. $L_y \approx 10$ nm and $L_z \approx 14$ nm for (b) and case (I) in (a). $L_y \approx 9$ nm and $L_z \approx 15$ nm for (d) and case (I) in (c). $L_y \approx 14.2$ nm, $L_z \approx 9.5$ nm for case (II) in (a) and (c). The widths of the nanowire are chosen to obtain a small critical Zeeman field for each case. (a,c) are obtained from the topological index $\mathcal{M} = -1$ (the filled regions). (c,d) are obtained from solving the BdG equation with $V_z = 1.5$ meV. $\Delta = 1$ meV. The dashed lines in (b,d) give the minigap. The parameters $\gamma_1, \gamma_2, \alpha$ are the same as that in Fig. 1b.

the phase boundary merge at $V_z = 0$, therefore the superconductor is gapped and topological for all V_z except at $V_z = 0$.

In the case (II), the threshold $V_z^c \approx p\Delta$ with $p = 2 \left[1 + 2 \left(1 + \beta_2^2 / \beta_1^2 \right)^{-1/2} \right]^{-1}$ (see Figs. 3a and 3c). For instance, for hole-doped InAs nanowires (with a typical $g_h^* = 35$ [30]) with Nb as the adjacent superconductor ($\Delta \simeq 1$ meV), the required magnetic field B is ~ 0.35 T, which is about 1/3 of the corresponding B for electron-doped InAs nanowires (with the same material Nb as the adjacent superconductor) [17], and can be easily realized with a bar magnet without affecting the superconducting pairing. Therefore, we find that irrespective of the relative sign of $\Delta_{s3/2}$ and $\Delta_{s1/2}$ (which can only be determined from a more microscopic calculation [26]) the threshold B for the TS state in the hole-doped case is much smaller than that in the electron-doped case. The fact that the Majorana fermions can be observed even with a small magnetic field opens the possibility of using a wide range of semiconductor materials with only small g_h^* factors [21, 22] and is one big advantage of using hole-doped semiconductors.

To further confirm the existence of the Majorana fermions in the above parameter regime, we also numerically solve the BdG equations (5) and obtain the energy

spectrum and eigenstates. The Majorana fermion corresponds to a zero energy eigenvalue in the BdG spectrum. Henceforth, we present our results only for the case (I), but have confirmed that the results for the case (II) are similar. In Fig. 3b, we plot the ground and the first excited state energies. The ground state energy becomes zero in the region $\mu_{c2} < \mu < \mu_{c1}$. In the same parameter region, the topological index $\mathcal{M} = -1$ (Fig. 3a), agreeing with the numerical results. The solution of the BdG equation also yields the minimum energy gap (minigap) above the zero energy states. At this gap and above there are other, finite-energy, states localized at the end points of the wire. The minigap therefore provides the protection for the Majorana states from finite temperature thermal effects. We see that the minigap is of the same order of the pairing gap $\Delta \simeq 1$ meV, which means that the Majorana fermion physics can be accessed at the experimentally accessible temperatures $T < 10$ K.

Effects of multiple confinement bands: In a realistic experiment, multiple confinement energy bands along the y and z directions need be taken into account [18, 31] because they are mixed with each other by the large spin-orbit coupling. Considering the lowest n confinement bands, the BdG Hamiltonian can be written as an $8n \times 8n$ matrix similar as Eq. (5) with the matrix elements replaced with the corresponding multiband forms. Specifically, $H_1(x)$ is replaced with $H_n(x) = \int dydz (\phi_1^*(y,z), \dots, \phi_n^*(y,z))^T H_L(\phi_1(y,z), \dots, \phi_n(y,z))$, where $\phi_i(y,z)$ is the wavefunction on the i -th band in the yz plane. Υ is replaced with $\Upsilon_n = I_n \otimes \Upsilon$. The Nambu spinor basis becomes $\hat{\Psi}(x) = (\hat{\psi}_1(x), \dots, \hat{\psi}_n(x), \Upsilon \hat{\psi}_1^\dagger(x), \dots, \Upsilon \hat{\psi}_n^\dagger(x))^T$ with $\hat{\psi}_i(x) = (\hat{\psi}_{\frac{3}{2}i}(x), \hat{\psi}_{\frac{1}{2}i}(x), \hat{\psi}_{-\frac{1}{2}i}(x), \hat{\psi}_{-\frac{3}{2}i}(x))^T$ as the hole annihilation operator on the i -th band. We also assume there is no superconducting pairing between holes at different confinement bands, therefore $\Delta_{Sn} = I_n \otimes \Delta_S$. Following a similar procedure as that for the single band, we derive the topological index $\mathcal{M} = \text{sgn}[\text{Pf}\{\Delta_{Sn} \Upsilon_n\} \text{Pf}\{\Upsilon_n \Delta_{Sn} + H_n^T(k) \Upsilon_n \Delta_{Sn}^{-1} H_n(k)\}]$ for the multiband model.

Here we consider only the lowest two relevant energy bands ($l_y = 1$ and $2, l_z = 1$). In Fig. 3c, we plot the parameter regime for the TS state when the multiple confinement induced bands are included. The parameter regime for the TS state now has some quantitative difference from that in the one-confinement-band case. However the basic conclusion remains the same, that is, the Majorana fermions can be realized even with very small Zeeman fields. In Fig. 3d, we plot the energies of the ground and first excited states by solving the relevant BdG equations in the multiband model. The figures confirm that the two methods – topological index and numerical solutions of BdG equations – yield the same results. In the multiband model, the minigap is slightly reduced, but still at the same order of Δ .

In practice, Δ may depend on the material as well

as the interface between the superconductor and the nanowire. Although the parameter regime for the emergence of Majorana fermions does not change much as a function of Δ , the minigap has a strong dependence on Δ . In Fig. 2b, we plot the minigap with respect to Δ in the multiband model and find that $E_g \sim \Delta$ (similar as the electron-doped case [15]), instead of Δ^2 as in a regular s -wave or a chiral- p wave superconductor. Therefore the minigap is rather large, which ensures thermal robustness of the Majorana fermions.

Conclusion: The list of systems capable of supporting a non-Abelian TS state now includes the filling factor $\nu = 5/2$ FQH state, chiral- p wave superconductors/superfluids, topological insulators, and electron-doped semiconductors. To this list we have added a new system, a *hole*-doped nanowire, as a possible non-Abelian platform. Although the roster is growing, ours is not an ordinary addition. As we have shown here in detail, the requirements (carrier density, magnetic field, g -factor, *etc.*) for the TS state in a hole-doped nanowire are *already accessible in experiments*. Thus this system can be a potential breakthrough facilitating solid-state demonstration of Majorana fermions as well as realization of TQC using a nanowire network.

Acknowledgements: We thank A. Akhmerov, F. Hassler, and M. Wimmer for helpful discussion on the form of the superconducting pairing. This work is supported by DARPA-MTO (FA9550-10-1-0497), DARPA-YFA (N66001-10-1-4025), ARO (W911NF-09-1-0248), and NSF-PHY (1104546).

* cwzhang@wsu.edu

- [1] G. Moore, and N. Read, Nucl. Phys. B **360**, 362 (1991).
- [2] C. Nayak, and F. Wilczek, Nucl. Phys. B **479**, 529 (1996).
- [3] N. Read, and D. Green, Phys. Rev. B **61**, 10267 (2000).
- [4] S. Das Sarma, M. Freedman, and C. Nayak, Phys. Rev. Lett. **94**, 166802 (2005).
- [5] D. A. Ivanov, Phys. Rev. Lett. **86**, 268 (2001).
- [6] S. Das Sarma, C. Nayak, and S. Tewari, Phys. Rev. B **73**, 220502(R) (2006).
- [7] G. E. Volovik, JETP Lett. **90**, 398 (2009).
- [8] M. A. Silaev and G. E. Volovik, J. Low Temp. Phys. **161**, 460 (2010).
- [9] S. Tewari *et al.*, Phys. Rev. Lett. **98**, 010506 (2007).
- [10] L. Fu, and C. L. Kane, Phys. Rev. Lett. **100**, 096407 (2008); *ibid* **102**, 216403 (2009); A. R. Akhmerov *et al.*, *ibid* **102**, 216404 (2009).
- [11] P. A. Lee, arXiv:0907.2681.
- [12] C. Nayak *et al.*, Rev. Mod. Phys. **80**, 1083 (2008).
- [13] J. D. Sau *et al.*, Phys. Rev. Lett. **104**, 040502 (2010).
- [14] J. Alicea, Phys. Rev. B **81**, 125318 (2010).
- [15] J. D. Sau *et al.*, Phys. Rev. B **82**, 214509 (2010).
- [16] Y. Oreg *et al.* Phys. Rev. Lett. **105**, 177002 (2010).
- [17] R. M. Lutchyn, J. D. Sau, and S. Das Sarma, Phys. Rev. Lett. **105**, 077001 (2010).
- [18] R. M. Lutchyn, T. D. Stanescu, and S. Das Sarma, Phys. Rev. Lett. **106**, 127001 (2011).
- [19] C. Zhang, *et al.* Phys. Rev. Lett. **101**, 160401 (2008).
- [20] A. C. Ford *et al.*, Nano Lett., **10**, 509 (2010).
- [21] M. Jeppsson *et al.*, J. Crys. Grow. **310**, 5119 (2008).
- [22] J. Xiang *et al.*, Nature Nano., **1**, 208 (2006).
- [23] S. Das Sarma *et al.*, Phys. Rev. Lett. **94**, 136401 (2005).
- [24] J. Sau, S. Tewari, and S. Das Sarma, arXiv:1111.2054.
- [25] B. A. Bernevig, and S.-C Zhang, Phys. Rev. Lett. **95**, 016801 (2005).
- [26] T. Stanescu *et al.*, to be published.
- [27] A. Yu. Kitaev, Phys. Usp. **44** (suppl.), 131 (2001).
- [28] P. Ghosh *et al.*, Phys. Rev. B **82**, 184525 (2010).
- [29] An anti-symmetric matrix $A = \begin{pmatrix} R & Q \\ -Q^T & S \end{pmatrix}$ can be diagonalized as $PAP^T = \begin{pmatrix} R & 0 \\ 0 & S + Q^T R^{-1} Q \end{pmatrix}$ with $P = \begin{pmatrix} I & 0 \\ Q^T R^{-1} & I \end{pmatrix}$. Here R , S , Q are matrices, I is a unit matrix.
- [30] V. Aleshkin *et al.*, Semiconductors **42**, 828 (2008).
- [31] A. C. Potter, and P. A. Lee, Phys. Rev. Lett. **105**, 227003 (2010).